IOP Publishing Journal of Physics G: Nuclear and Particle Physics
J. Phys. G: Nucl. Part. Phys. **42** (2015) 034007 (18pp) doi:10.1088/0954-3899/42/3/034007

Statistical methods for thermonuclear reaction rates and nucleosynthesis simulations

Christian Iliadis[1,2], Richard Longland[2,3], Alain Coc[4], F X Timmes[5] and Art E Champagne[1,2]

[1] University of North Carolina at Chapel Hill, Chapel Hill, NC 27599-3255, USA
[2] Triangle Universities Nuclear Laboratory, Durham, NC 27708-0308, USA
[3] North Carolina State University, Raleigh, NC 27695, USA
[4] Centre de Sciences Nucléaires et de Sciences de la Matière (CSNSM), CNRS/IN2P3, Université Paris Sud 11, UMR 8609, Bâtiment 104, F-91405 Orsay Campus, France
[5] School of Earth and Space Exploration, Arizona State University, Tempe, AZ 85287-1504, USA

E-mail: iliadis@unc.edu

Received 28 May 2014, revised 6 August 2014
Accepted for publication 12 August 2014
Published 5 February 2015

Abstract

Rigorous statistical methods for estimating thermonuclear reaction rates and nucleosynthesis are becoming increasingly established in nuclear astrophysics. The main challenge being faced is that experimental reaction rates are highly complex quantities derived from a multitude of different measured nuclear parameters (e.g., astrophysical S-factors, resonance energies and strengths, particle and γ-ray partial widths). We discuss the application of the Monte Carlo method to two distinct, but related, questions. First, given a set of measured nuclear parameters, how can one best estimate the resulting thermonuclear reaction rates and associated uncertainties? Second, given a set of appropriate reaction rates, how can one best estimate the abundances from nucleosynthesis (i.e., reaction network) calculations? The techniques described here provide probability density functions that can be used to derive statistically meaningful reaction rates and final abundances for any desired coverage probability. Examples are given for applications to s-process neutron sources, core-collapse supernovae, classical novae, and Big Bang nucleosynthesis.

Keywords: thermonuclear reaction rates, nucleosynthesis, statistical methods, Monte Carlo, stellar models

(Some figures may appear in colour only in the online journal)

1. Introduction

Our understanding of the Universe has been revolutionized by new observational technologies. Advances in detectors, computer processing power, network bandwidth, and data storage capability have enabled new sky surveys (e.g., the *Sloan Digital Sky Survey* [1]). Advances have triggered many new optical transient surveys (e.g., the *Palomar Transient Factory* [2, 3]) that probe ever larger areas of the sky and ever-fainter sources, opening up the vast discovery space of time-domain astronomy. Advances have also allowed for space missions, for example, NASA's *Kepler* [4, 5], that continuously monitor more than 100 000 stars. The discoveries from these surveys include revelations about stellar nucleosynthesis, unusual explosion outcomes, and remarkably complex binary star systems. The immediate future holds tremendous promise, as both the space-based survey *Gaia* and the ground based *Large Synoptic Survey Telescope* come to fruition.

Many forefront questions in astrophysics ultimately require a detailed quantitative knowledge of stellar properties, thus challenging stellar models to become more sophisticated, quantitative and realistic in their predictive power (e.g., *Modules for Experiments in Stellar Astrophysics* [6, 7]). This in turn requires more detailed physics input, such as thermonuclear reaction rates and opacities, and a concerted effort to validate models through systematic observations. The study of nuclear reactions in the observable Universe remains at the forefront of nuclear physics and astrophysics research. On the nuclear physics side, data on cross sections and nuclear properties of astrophysically important reactions are being obtained at radioactive ion-beam facilities and at stable-beam facilities at an accelerated pace (e.g., *Facility for Rare Isotope Beams* [8]). Radiation detectors, ion beam technology, and low-background techniques have reached an unprecedented stage of sophistication, permitting measurements of increasing precision and sensitivity (e.g., *Laboratory for Experimental Nuclear Astrophysics* [9, 10].) We recognize that insight can be gained in observational astronomy and nuclear astrophysics by acquiring new information about atomic nuclei and by recognizing the importance of what needs to be measured in the laboratory.

Thermonuclear reaction rates are at the heart of every Big Bang and stellar model. In the following we will discuss statistical techniques for deriving reliable reaction rates and their associated uncertainties. This approach is useful for assessing which nuclear properties of a given reaction need to be measured in the laboratory, and for identifying the most important nuclear reactions that impact a given isotopic abundance during nuclear burning in stars.

Experimental thermonuclear reaction rates, based on nuclear physics input gathered from laboratory measurements, were first presented by Willy Fowler and collaborators more than 40 years ago ([11], and references therein). Those reaction rates were directly based on nuclear physics experiments and were distinct from reaction rates derived from theory (e.g., the Hauser–Feshbach model). The incorporation of Fowler's rates into stellar models represented a paradigm shift for astrophysics. With a solid nuclear physics foundation, stellar simulations could provide reasonable estimates of nuclear energy generation and nucleosynthesis. Subsequent work [12, 13] incorporated newly measured nuclear physics data, but the reaction rates were still computed using techniques developed prior to 1988.

The main challenge with such approaches in the modern era, is that thermonuclear reaction rates are reported as single value at a given temperature, without any uncertainty estimate, or that a recommended rate is presented together with 'limits'. These upper and lower rate limits are frequently obtained by inclusion or exclusion of unobserved low-energy resonances. Such reaction rate limits are a drawback in the modern era since they lack a rigorous statistical meaning. Specifically, since the reaction rate probability density function remains unknown with these methods, the reported rate limits cannot be quantified in terms of

a coverage probability. A significant obstacle to overcome in this regard is the fact that thermonuclear reaction rates are highly complex quantities derived from a multitude of nuclear physics properties painstakingly extracted from laboratory measurements (resonance energies and strengths, non-resonant cross sections, spectroscopic factors, etc.)

2. Monte-Carlo based reaction rates

2.1. Method

One approach to addressing these challenges is described in [14–18]. The method is conceptually straightforward and follows a Monte Carlo procedure. First, all of the measured nuclear physics (input) properties entering into the reaction rate calculation are randomly sampled according to their individual probability density functions. Second, the sampling is repeated many times and thus provides the Monte Carlo reaction rate (output) probability density. Third, the associated cumulative distribution is determined and is used to derive reaction rates and their uncertainties with a precise statistical meaning (i.e., a quantifiable coverage probability). For example, for a coverage probability of 68%, the low, recommended, and high Monte Carlo rates can be defined as the 16th, 50th, and 84th percentiles, respectively, of the cumulative reaction rate distribution[6]. The main challenge is to randomly sample all nuclear physics input parameters, including resonance energies and strengths, partial widths, reduced widths, astrophysical S-factors, etc., according to physically motivated probability density functions [15].

Depending on the nature of the nuclear physics observable, the (input) probability densities should be chosen according to the central limit theorem of statistics. It states that the sum of n independent continuous random variables x_i, with means μ_i and standard deviations σ_i, becomes a normal (Gaussian) random variable in the limit of $n \to \infty$, independent of the form of the individual probability density functions of the x_i. Many measurement uncertainties are treated as Gaussian random variables if it can be assumed that the total uncertainty is given by the sum of a large number of small contributions. This is usually the case for measured resonance energies, with contributions from the beam energy calibration, the measured yields, the fitting of the yield curve to find the 50% point, target inhomogeneities, dead layers, etc.

It also follows directly from the central limit theorem that a random variable will be distributed according to a lognormal density function if it is determined by the product of many factors. This is usually the case for experimental resonance strengths (i.e., integrated resonance cross sections), which are determined from the measured number of counts of a thick-target yield, the integrated beam charge, a detector efficiency, a stopping power, etc. The lognormal distribution is given by

$$f(x) = \frac{1}{\sigma\sqrt{2\pi}}\frac{1}{x}\mathrm{e}^{-(\ln x-\mu)^2/(2\sigma^2)} \tag{1}$$

and is defined by the two parameters μ and σ. The first parameter μ determines the location of the distribution, while the second parameter σ controls the width. An exhaustive account of this method can be found in [15].

As an example, we show in figure 1 the experimental Monte Carlo based rate of the ^{22}Ne $(\alpha,\mathrm{n})^{25}$Mg reaction at a temperature of 300 MK, which is a key neutron source for the

[6] N sampled values of reaction rates, x_i, are sorted into ascending order and the percentile, q, is found from the fraction of values located below a given value of x_q.

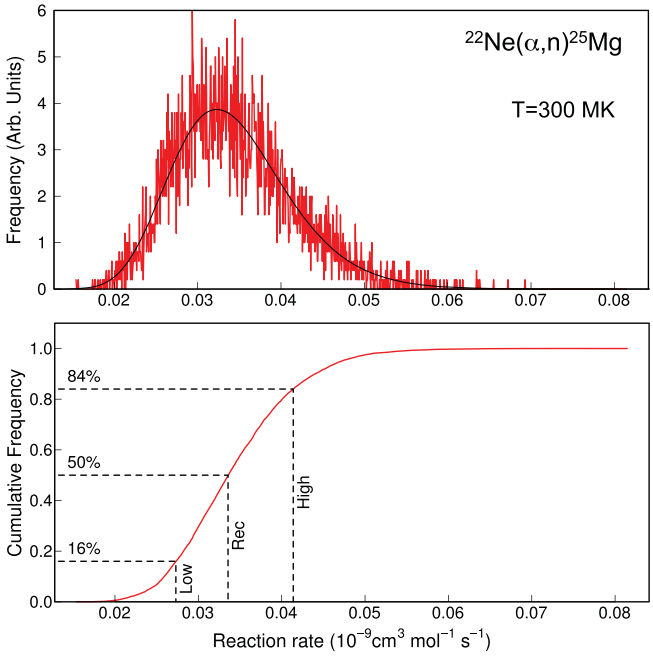

Figure 1. Experimental Monte Carlo based reaction rates for the crucial ^{22}Ne(α,n)^{25}Mg neutron source in the s-process at a temperature of 300 MK [19]. The rate is obtained by sampling 166 different nuclear parameters (resonance energies and strengths, α-particle, neutron, and γ-ray partial widths), and the Monte Carlo sampling is repeated 10 000 times. (Top) Reaction rate probability density function, shown in red; the black solid line represents a lognormal approximation, which is directly obtained from the mean and variance of the Monte Carlo rate samples (i.e., no fitting is involved). (Bottom) Cumulative reaction rate distribution; notice the much reduced scatter. The vertical dotted lines represent the low, median and high Monte Carlo reaction rates, which are obtained from the 16th, 50th and 84th percentiles, respectively. From [51].

astrophysical s-process that occurs during helium burning in AGB stars and massive stars. The total reaction rate has contributions from 23 resonances with measured energies and resonance strengths or partial widths, and from 19 resonances for which only upper limits on the partial widths are available. In total, 166 different nuclear parameters (resonance energies and strengths; α-particle, neutron, and γ-ray partial widths) are randomly sampled to estimate this particular rate. The upper and lower panels of the figure display the Monte Carlo probability density function and the associated cumulative distribution, respectively, of the *experimental* rate at a stellar temperature of 300 MK. The 16th, 50th, and 84th percentiles, indicated in the lower part, define one particular choice for the reaction rate uncertainty, corresponding to a coverage probability of 68%. The Monte Carlo based rate of this reaction differs significantly from previously published results. Details can be found in [19]. The Monte Carlo probability density is a smoothly varying function, without any sharp boundaries, challenging previous definitions of an 'upper limit' or 'lower limit' for a reaction rate.

Reaction rates based on the Monte Carlo method do not consider only *statistical* uncertainties in the nuclear physics input, since the Monte Carlo sampling does not distinguish between statistical and systematic effects. For example, suppose a reported experimental value for a resonance strength amounts to 5.0 ± 0.5 eV. Closer scrutiny of the

experimental technique may reveal that certain systematic effects were not taken into account. Perhaps the detection efficiency was not corrected for coincidence summing effects, or older stopping power values were employed. If such systematic effects can be accounted for by adjusting the reported mean value and the uncertainty, the nuclear input to the Monte Carlo procedure will represent the *best estimate* based on known statistical and systematic effects. Of course, unknown systematic effects may still impact the total rate.

A public web-portal interface to a RatesMC executable [15][7] allows users to calculate experimental Monte Carlo based rates. The current version of the code is applicable to many nuclear reactions provided that the total rates are determined by the incoherent contributions of any number of broad or narrow resonances and of up to two non-resonant (i.e., direct) amplitudes. The code also accounts for interferences between any two resonant amplitudes. Interferences of more than two resonant contributions, or between a resonant and a non-resonant amplitude, have not been implemented yet.

Many correlations between nuclear quantities are considered carefully in RatesMC. For example, if the strength of a narrow resonance is estimated from a reduced width or a spectroscopic factor, then the uncertainty in the resonance energy enters both in the Boltzmann factor and in the penetration factor. Thus the same random value of the resonance energy, drawn from a Gaussian probability density function, must be used in both expressions. Other correlations are not yet considered in RatesMC, although their implementation is straightforward from a computational point of view. For example, the same partial width value may enter in the rate expressions of two competing reactions involving the same target nucleus. In this case, the same random value of the width, drawn from a lognormal probability density function, should be used for both reactions. We will consider such improvements in a future release of RatesMC.

It is apparent that in example of figure 1 the rate probability density can be approximated by a lognormal distribution, shown as the black solid line in the top panel of figure 1. We find that this is the case for the majority of Monte Carlo based reaction rates at most stellar temperatures of interest. A detailed discussion is presented in [16]. We will return to this point below, which is crucial for how to implement the new Monte Carlo based reaction rates in nucleosynthesis studies.

2.2. Upper limits of nuclear physics input parameters

Many reaction rates have contributions from unobserved low-energy resonances. More precisely, levels are known to exist near the projectile threshold energy, but the corresponding resonances have not been observed directly in the laboratory yet. At low bombarding energies, proton or α-particle partial widths are dominated in magnitude by the transmission through the Coulomb barrier and thus are usually much smaller compared to γ-ray partial widths. For example, in the simple case of a low energy resonance with only one particle channel and the γ-ray channel open, the resonance strength that enters into the calculation of the reaction rate is given by

$$\omega\gamma \equiv \omega\frac{\Gamma_x\Gamma_\gamma}{\Gamma} \approx \omega\Gamma_x = 2\frac{\omega\hbar^2}{\mu R^2}P_\ell\theta_x^2, \tag{2}$$

with Γ_x, Γ_γ, Γ the particle partial width, γ-ray partial width, and total width, respectively; μ, R, P_ℓ, and θ_x^2 denote the reduced mass, channel (nuclear) radius, penetration factor, and dimensionless reduced width, respectively; furthermore, $\omega \equiv (2J_r + 1)/[(2j_p + 1)(2j_t + 1)]$,

[7] See http://starlib.physics.unc.edu.

where J_r, j_t, j_p are the spins of the resonance, target, and projectile, respectively. In simple terms, the penetration factor represents the nuclear exterior and can be computed from numerical values of Coulomb wave functions. The only unknown quantity in the above expression, assuming that J^π is known, is the dimensionless reduced width, which describes the nuclear interior[8]. The question arises of how to implement such contributions into the Monte Carlo sampling procedure if only an upper limit for θ_x^2 is available, either from experiment or from theory.

A solution to this problem is closely related to fundamental predictions of random matrix theory. The basic assumption is that energy levels in atomic nuclei at several MeV excitation energies represent chaotic systems. The reduced width amplitude for formation or decay of an excited compound nucleus is assumed to be a random variable, with many small contributions from different parts of configuration space. If the contributing nuclear matrix elements are random in magnitude and sign, the reduced width amplitude is represented by a Gaussian probability density centered at zero, according to the central limit theorem (section 2.1). Consequently, the corresponding reduced width, i.e., the square of the amplitude, is described by a chi-squared probability density with one degree of freedom,

$$g\left(\theta^2\right) = \frac{1}{\sqrt{2\pi\theta^2\left\langle\theta^2\right\rangle}} \mathrm{e}^{-\frac{\theta^2}{2\left\langle\theta^2\right\rangle}} \tag{3}$$

with $\langle\theta^2\rangle$ the local mean value of the dimensionless reduced width. This expressions is known as the Porter–Thomas distribution [21]. It implies that the reduced widths for a single reaction channel, i.e., for a given nucleus and set of quantum numbers, vary by several orders of magnitude, with a higher probability for smaller values of the reduced width. Until recently this fundamental prediction of random matrix theory had been disregarded in nuclear astrophysics. It was shown in [16, 17] that a proper treatment of the contributions from unobserved resonances, based on the Porter–Thomas distribution, can change the estimated total thermonuclear reaction rate by orders of magnitude compared to previous predictions.

The crucial ingredient for the Monte Carlo sampling of an upper limit contribution according to the Porter–Thomas distribution is the mean value of the reduced width, $\langle\theta^2\rangle$. It is not predicted by random matrix theory, but can be obtained from the analysis of laboratory data or from a suitable nuclear reaction model[9]. A first step in this direction was the recent extraction [22] of mean reduced widths from high-resolution data measured at Triangle Universities Nuclear Laboratory (TUNL) for target mass ranges of $A = 28 - 40$ (α-particles) and $A = 34 - 67$ (protons). For example, a mean value of $\langle\theta_\alpha^2\rangle = 0.018$, averaged over target nuclei, spin-parities, and excitation energies, was obtained for α-particles, almost a factor of two larger than the preliminary value suggested in [15].

An example for the relevance of these results is given in figure 2. The calculated experimental Monte Carlo-based rates for the ^{40}Ca(α,γ)^{44} Ti reaction, which is crucial for the production of the γ-ray emitter ^{44}Ti in core-collapse supernovae [23–30] are shown as a contour plot (black-red-yellow; see color bar on the right). The colors signify the coverage probability between any given rate boundaries. The rates are normalized to the recommended Monte Carlo rate for a better comparison. For example, the thick (thin) black lines indicate the high and low Monte Carlo rates for a coverage probability of 68% (95%). The blue and green

[8] The dimensionless reduced width is closely related to the spectroscopic factor, see [20].

[9] The mean reduced width is related to the strength function of channel c via $s_c^J \equiv \langle\gamma_{\lambda c}^2\rangle / D^J$, where D^J is the mean energy spacing for compound levels of spin J; the reduced width, γ^2, and dimensionless reduced width, θ^2, are related by $\gamma^2 \equiv (\hbar^2/(\mu R^2))\theta^2$, with μ the reduced mass and R the channel radius. The strength function determines the transmission coefficient, which is a key quantity for estimating average nuclear reaction cross sections.

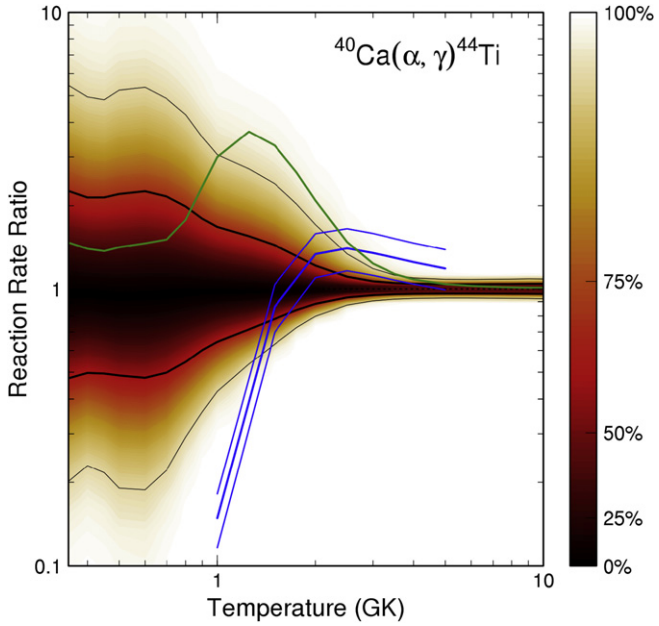

Figure 2. Monte Carlo-based reaction rates of ^{40}Ca(α,γ)^{44}Ti. For a better comparison, the rates are normalized to the recommended Monte Carlo rate. The color-shading indicates the coverage probability in percent. The thick (thin) black lines indicate the high (low) Monte Carlo rates for a coverage probability of 68% (95%). Note that the Monte Carlo rate has no sharp bounderies (i.e., no 'lower limit' or 'upper limit'), but instead is represented by a smoothly varying probability density function along the ordinate. The blue and green lines show the rates obtained using conventional (i.e., pre-Monte Carlo) methods. Reproduced with permission from [22]. Copyright 2013 by the American Physical Society.

lines show the rates obtained by using conventional (i.e., pre-Monte Carlo) methods: (blue) results of [31], where the unobserved low-energy resonances were disregarded; (green) upper limit obtained if the maximum contribution of the unobserved resonance at $E_\alpha^{c.m.} = 2373$ keV is adopted. It is apparent that the new Monte Carlo rates are significantly different from previous results.

So far, the only systematic analysis of mean values for dimensionless reduced widths has been presented by Pogrebnyak *et al* [22]. As already mentioned, these values were extracted from the available experimental data for a range of compound nuclei, A, spin-parities, J^π, and excitation energies, E_x. However, the experimental values cover only a small part of the A-J^π-E_x parameter space and it is highly desirable to have access to $\langle\theta^2\rangle$ values for all cases of interest. Considering that the data analyzed in [22] were accumulated over a period of more than 40 years at the now decommissioned high-resolution 3-MeV Van de Graaff accelerator laboratory at TUNL, it is clear that the desired $\langle\theta^2\rangle$ values need to be obtained from nuclear theory, for example, using the shell model. Additional efforts are needed in this direction.

2.3. Individual contributions to the total reaction rate

Suppose a given nuclear reaction has been identified as a key process for some astrophysical environment and that an experimentalist intends to measure this reaction. The immediate questions at hand are: what energy range should be covered in the laboratory? And which

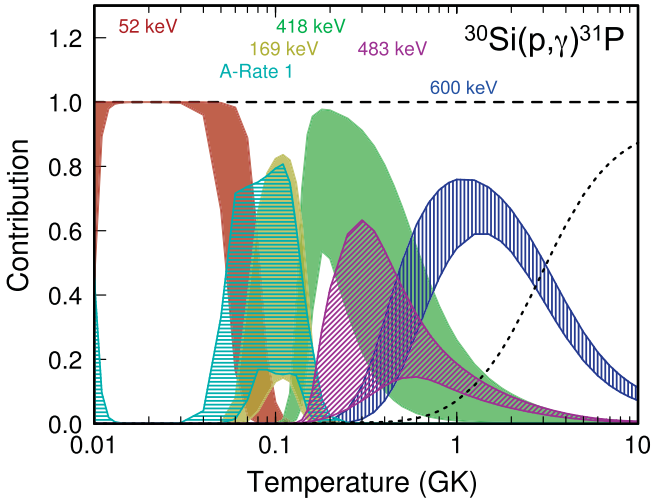

Figure 3. Fractional contributions to the total ^{30}Si(p,γ)^{31}P reaction rate. Different colors indicate different contributions. The vertical width of a band, indicating the uncertainty of a fractional contribution, has a precise statistical meaning—a coverage probability of 68%. The results are obtained from the Monte Carlo based method described in the text. Numbers at the top denote center-of-mass energies of given resonances; 'A-Rate 1' refers to the non-resonant (direct capture) rate contribution; the dotted line shows contributions of resonances with energies larger than 600 keV. From [51].

nuclear properties should, in fact, be measured? The usual approach is to determine first the temperature range of astrophysical interest, then to convert the temperatures to a range of bombarding energies with the help of the Gamow peak concept [32], and then to address this energy region with direct or indirect measurements. However, there are pitfalls associated with using the Gamow peak concept, as pointed out by [33, 34]. This procedure can only be regarded as a rough estimate, partly because previously published reaction rates have no rigorous statistical meaning and partly because it is difficult to disentangle the impact of different nuclear physics input parameters (resonance energies, strengths, partial widths, spectroscopic factors, etc.) and their associated uncertainties on the total reaction rate.

The availability of Monte Carlo based reaction rates opens a new window of opportunity. Since each nuclear physics input parameter is sampled according to a physically motivated probability density function [15], the Monte Carlo sampling provides a statistically rigorous coverage probability for each contribution. As an example, consider figure 3, showing the main fractional contributions of individual observed or unobserved resonances to the total ^{30}Si(p,γ)^{31}P Monte Carlo reaction rate. This reaction is of particular interest for interpreting observed silicon isotopic ratios in nova candidate presolar grains [35]. Different colors correspond to contributions of different resonances, while the vertical width of each band signifies a coverage probability of 68%. Inspection of the figure clearly identifies what needs to be measured in order to improve the total reaction rate estimate, without resorting to the Gamow peak concept. For example, at typical classical nova peak temperatures near 300 MK the total rate is dominated by the uncertainties in the contributions of the 418 keV and the 483 keV resonances. The former has not been directly observed yet, while the latter has been observed, albeit with a large uncertainty in the experimental resonance strength.

Fractional reaction rate contributions, computed using the Monte Carlo method, will play an important role for the design of future measurements at existing or planned nuclear physics

laboratories since they identify the rate contributions to be measured and indicate the degree of experimental precision required.

2.4. STARLIB: a new nuclear rate library for stellar modeling

The solid black line in the top panel of figure 1 represents a lognormal function that closely describes the actual Monte Carlo reaction rate probability density shown as the red histogram. It was found in [16] that lognormal distributions provide a useful approximation for the majority of the reaction rate probability densities. This aspect is interesting because, as discussed above, a lognormal function is defined by only two parameters, μ and σ. The first parameter is related to the *median rate* via $x_{\rm med} = e^{\mu}$, while the second parameter is related to the *factor uncertainty with respect to the median* via $f.u. = e^{\sigma}$ (for a coverage probability of 68%). Therefore, by tabulating values for temperature, T, recommended rate, $x_{\rm med}$, and factor uncertainty, $f.u.$, the rate probability density function can be computed conveniently by using equation (1) at any temperature bounded by the table entries.

These ideas are crucial for the design of a next-generation reaction rate library, called STARLIB [36]. Existing libraries contain values of only two quantities, i.e., temperature and recommended rate, either as analytical fit formulas (e.g., JINA REACLIB or BDAT [37]) or in tabular format (e.g., BRUSLIB [38]). STARLIB also uses a tabular format, providing temperature and recommended rate, but in addition lists the factor uncertainty as a third parameter, which can be used for two purposes. First, it provides an estimate for the rate uncertainty since the coverage probability for rate values between $x_{\rm low} = e^{\mu}/e^{\sigma} = x_{\rm med}/(f.u.)$ and $x_{\rm high} = e^{\mu}e^{\sigma} = x_{\rm med}\,(f.u.)$ is 68%. Second, the listed values for $x_{\rm med}$ and $f.u.$ determine the entire rate probability density function, as discussed above. This aspect is important because it allows for a convenient implementation of Monte Carlo based reaction rates in nucleosynthesis studies, as will be discussed in the next section. Experimental Monte Carlo based thermonuclear reaction rates are so far available for about 70 nuclear reactions involving target nuclei in the $A = 14$–40 range. Experimental β-decay rates, including their lognormal decay constant probability densities, are easily incorporated into the structure of STARLIB [36].

A general-purpose nuclear reaction and decay library must also encompass tens of thousands of nuclear interactions for which no experimental information exists. For these reactions, STARLIB contains theoretical rates that are computed using the nuclear reaction code TALYS.[10] Reliable uncertainties for theoretical reaction rates are difficult to assess at present. Various claims have been made in the literature ('on average within a factor of two'), which may be optimistic. Traditionally, such uncertainties have been systematically evaluated using reaction codes by exploring different sets of nuclear input models for each target and each reaction channel. A similar approach could be followed to estimate the uncertainties affecting the TALYS rates. However, the present version of STARLIB adopts a recommended factor of 10 uncertainty for any reaction rate for which no experimental cross section information exists. This value represents currently our best estimate based on experience. The factor uncertainty, together with the recommended rate, is used to compute the lognormal rate probability density for TALYS-based rates in the same manner as for the experimental Monte Carlo rates discussed above. One of the future goals is to replace many of the theoretical rates with experimental Monte Carlo-based estimates. A detailed discussion of the publicly available STARLIB reaction rate library[11] is given in [36].

[10] See http://www.talys.eu.
[11] See http://starlib.physics.unc.edu.

3. Monte carlo nucleosynthesis

STARLIB contains the rate probability densities of all reactions in the network. Therefore, the obvious next step is to employ these rates in Monte Carlo nucleosynthesis studies. Notice that we are referring to two different Monte Carlo procedures: the first is used to derive reaction rates by randomly sampling over the experimental nuclear physics input, as described in the previous section (step 1), while the second refers to estimating abundances by randomly sampling over the reaction rates, as will be discussed below (step 2). This method is flexible, in the sense that all reaction rates can be varied simultaneously, or specific groups of reactions can be studied separately. Here we will concentrate on the former case. The general strategy is to randomly sample the rates for every reaction in the network and to compute a single nucleosynthesis model. The procedure is repeated many times to collect an ensemble of abundances from different reaction network runs, which can then be further analyzed. It should be emphasized that pairs of corresponding forward and reverse rates should *not* be sampled independently since they are correlated according to the reciprocity theorem. The proper sampling procedure in this case has been discussed in detail by [36].

Monte Carlo nucleosynthesis studies have been performed previously (e.g., [39–41]), but did not use statistically meaningful rate probability density functions derived from experimental nuclear physics input. Instead, previous studies, as is common practice, assigned arbitrary 'enhancement' factors to the rates. In most cases, these enhancement factors were globally defined by identifying the type of reaction rate (e.g., whether from experimental data, or purely from theory). In particular, these enhancement factors were assumed to be independent of temperature. Given the discussion of Monte Carlo reaction rates in section 2, it is clear that this assumption is not valid in general. Rather, the rate uncertainties display a strong temperature-dependence arising from different resonance contributions (see, for example, figure 2) and hence the temperature dependence must be considered carefully in the sampling procedure.

One choice for performing Monte Carlo nucleosynthesis studies (step 2) is to utilize directly the random samples of the Monte Carlo reaction rates (step 1). The advantage of this choice is that the individual rate samples are directly based on the nuclear physics input and thus will account for all possible behaviors of reaction rates as a function of temperature. The disadvantage is that it requires a considerable amount of effort, along with a detailed knowledge of all nuclear physics input not widely available to users. Therefore, we describe below a reaction rate sampling method that is simpler to implement and agrees well with more complex choices [42].

3.1. Reaction rate sampling

Most reactions for which we have computed Monte Carlo-based rates so far are dominated by resonances. In the absence of interference effects, the individual resonant contributions are summed incoherently to obtain the total reaction rate. Therefore, reactions that involve a large number of resonances with uncorrelated uncertainties may exhibit complex rate variations from random sample to sample. One important physical constraint is that these reaction rates must be a smooth function of temperature owing to the convolution of the nuclear reaction cross section with the thermal energy distribution of the particles in the stellar plasma.

The two parameters, lognormal μ and σ, define the approximate reaction rate probability density function. These parameters form the basis of our sampling scheme. For a lognormal probability density, a random rate sample, $x(T)$, at a specific temperature, T, is computed from

$$x(T) = \mathrm{e}^{\mu(T)} \times \mathrm{e}^{p(T)\sigma(T)} = x(T)_{\mathrm{med}} \times (f.u.(T))^{p(T)}, \quad (4)$$

where $x_{\mathrm{med}}(T) = \mathrm{e}^{\mu(T)}$ and $f.u.(T) = \mathrm{e}^{\sigma(T)}$ are the median rate and factor uncertainty (section 2.4), respectively, and $p(T)$ is a random variable that is normally distributed, i.e., according to a Gaussian distribution with an expectation value of zero and standard deviation of unity. Note that $(f.u.(T))^{p(T)}$, and not $p(T)$, is the factor by which the sampled reaction rate is modified from its median value. The former factor depends on temperature through both $(f.u.(T))$ and $p(T)$. With the lognormal parameters, $\mu(T)$ and $\sigma(T)$, given in STARLIB, sampling over reaction rates becomes a simple task of assuming an appropriate sampling scheme for the random variable $p(T)$.

The simplest parameterization for $p(T)$ is obtained by assuming that it is independent of temperature, i.e., $p(T) = a$, where a is sampled from a normal distribution. This parameterization was found to reproduce the abundance uncertainties arising from more complex sampling schemes [42]. Even in this simplest case the rate uncertainty factor, given by $\mathrm{e}^{a\,\sigma(T)}$ in equation (4), is still temperature dependent. This temperature dependence was disregarded in previous Monte Carlo studies (e.g., [40]) that employed a constant, temperature-independent value for the uncertainty factor. Figure 4 illustrates this point, showing that a uniform value of $p(T) = a$ produces a rate sample with a temperature-dependent uncertainty. In the following we will refer to $p(T) = a$ as the *rate variation factor*.

3.2. Nucleosynthesis studies

A Monte Carlo study of the nucleosynthesis can be performed following these steps: (i) for each (forward) reaction, the normally distributed variables, p_i, are sampled independently; (ii) the rates obtained are used to compute the nucleosynthesis for a single post-processing network run; (iii) steps (i) and (ii) are repeated a sufficient number of times to obtain an ensemble of final nucleosynthesis abundance yields. The Monte Carlo procedure has major advantages compared to varying rates one-by-one in sequential network runs. On the one hand, it is straightforward to derive from the ensemble of final Monte Carlo abundances the recommended values and associated uncertainties. One choice is to adopt the 16th, 50th, and 84th percentiles as the low, recommended, and high abundance, respectively, similar to the recipe discussed in connection with reaction rates (section 2.1). On the other hand, the impact of a given reaction rate uncertainty on the nucleosynthesis can be easily quantified by storing the values of p_i for each sample reaction network run. A scatter plot of the final abundance for a given nuclide versus the sampled value of p_i can then be investigated for correlations.

In order to illustrate these points, we will apply in the following the Monte Carlo method to Big Bang nucleosynthesis. Observations of primordial ^{4}He, ^{2}H and ^{7}Li abundances have reached an unprecedented level of precision. Therefore, reliable predicted abundances are needed before the observations can be confronted with theory. Such studies have interesting implications for testing standard or non-standard Big Bang models, since Big Bang nucleosynthesis represents the earliest milestone of known physics when we look back in time. The nucleosynthesis problem is also well-defined, in the sense that the number of nuclear reactions in the network is relatively small. Furthermore, the temperature and density evolution during the Big Bang can be calculated from first principles and hence the results are independent of convection, mass loss, opacities, magnetic fields, etc., which introduce additional uncertainties to stellar nucleosynthesis predictions. Numerous studies (see, e.g., [43]) have shown that the predicted Big Bang abundances of the light elements, for example, ^{2}H and ^{4}He, agree with the observations. The sole exception is ^{7}Li, which is overproduced by a factor of three relative to observations. The ^{7}Li problem represents the central unsolved

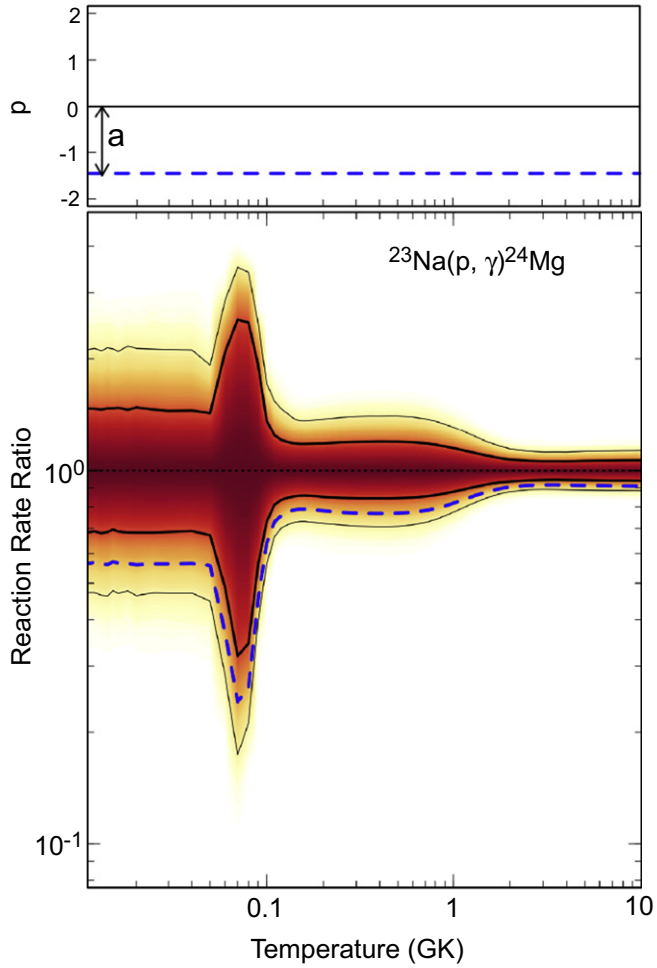

Figure 4. Reaction rate ratio (i.e., normalized to the recommended rate) for the ^{23}Na(p, γ)^{24}Mg reaction, obtained using the Monte Carlo method discussed in section 2.1. The color indicates the coverage probability of the rate density function. The thick and thin black lines correspond to 68% and 95% rate uncertainties, respectively, similar to figure 2. The dashed blue line represents a single reaction rate sample obtained with equation (4) and $p(T) = a$. From [51].

puzzle of the nucleosynthesis in the early Universe. A solution is actively sought either in observation, nuclear physics, or new physics beyond the standard model [44].

Results from the Monte Carlo procedure are shown in figure 5. The reaction network includes 59 nuclides between the neutron and Na, and consists of 424 nuclear interactions [45]. It is much larger than in other studies of standard Big Bang nucleosynthesis because it is designed to study weak flows into the CNO region. For this network, the rates of all reactions, except for reverse reactions (section 3), are independently sampled. In other words, each rate is multiplied by a temperature-independent random variation factor, p_i, and thus is sampled according to a temperature-dependent lognormal probability density function (equation 4). The sampling is repeated for 30 000 reaction network runs. The histogram of all 30 000 final number abundance ratios ^{7}Li/H is displayed in the left panel of figure 5. Note that ^{7}Li is

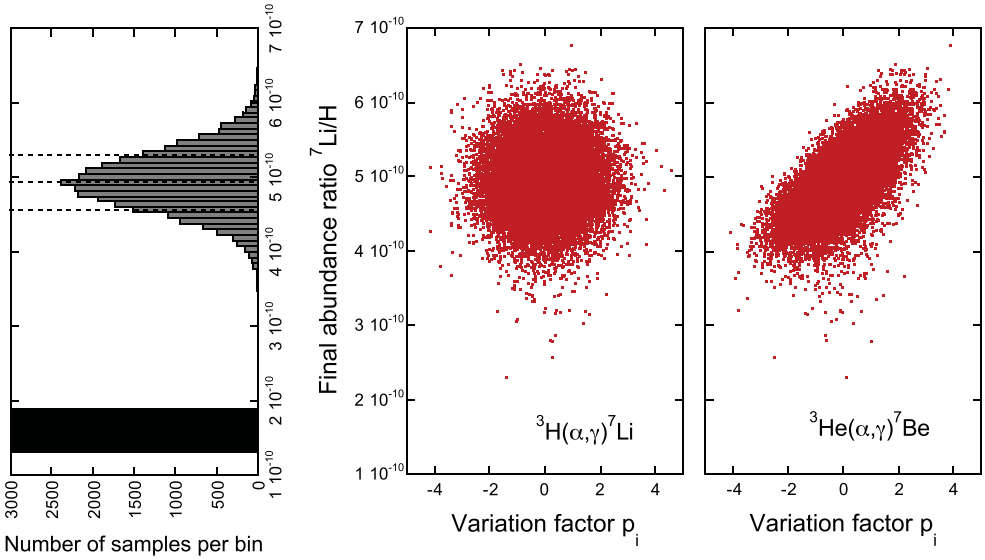

Figure 5. Results of a Monte Carlo study of Big Bang nucleosynthesis, using 30 000 reaction network runs. (Left) Histogram of final ^{7}Li/H number abundance ratio; the dashed lines indicate the 16th, 50th, and 84th percentiles of the abundance distribution; the observed range is indicated by the black bar. (Middle) Final ^{7}Li/H number abundance ratio versus variation factor of the ^{3}H(α,γ)^{7}Li rate. (Right) Final ^{7}Li/H number abundance ratio versus variation factor of the ^{3}He(α,γ)^{7}Be rate. The scatter plot in the middle panel shows no correlation, while a strong correlation is apparent in the right panel. The projection of either scatter plot on the ordinate results in the panel shown on the left.

mainly produced in the Big Bang as ^{7}Be, which quickly decays to ^{7}Li. This indirect Big Bang synthesis of ^{7}Li exceeds the direct synthesis by a factor of about 20. The dashed lines represent the 16th, 50th, and 84th percentiles, which amount to ^{7}Li/H = 4.56×10^{-10}, 4.94×10^{-10}, and 5.34×10^{-10}, respectively. These values are based on our best estimates for the probability density functions of all reaction rates in the network, including all *known statistical and systematic effects* (section 2.1). As already noted, the observations result in a factor of three smaller ^{7}Li/H ratio, indicated by the black bar in the lower part of the left panel. Thus it is unlikely that the solution of the ^{7}Li problem will be found in uncertain nuclear physics. This conjecture disregards *unknown systematic effects*.

The next question at hand is: which reaction rates have the strongest impact on the predicted ^{7}Li/H ratio? Once identified, these reactions can be subjected to further scrutiny and the experimental data can be inspected for previously unaccounted systematic effects. The Monte Carlo results presented above contain an answer to this question since the variation factors, p_i, of each reaction are recorded for each of the 30 000 network calculations. Consider again figure 5, displaying the final ^{7}Li/H ratios of all 30 000 network runs versus the sampled rate variation factors, p_i, of ^{3}H(α,γ)^{7}Li (middle panel) and ^{3}He(α,γ)^{7}Be (right panel). The projection of any of these scatter plots onto the ordinate results in the (same) histogram shown on the left, which was already discussed above. Again, the spread along the y-direction is caused by the combined uncertainties of all reaction rates in the network. The impact of a given reaction rate on the final abundance of a given nuclide, X_f, is apparent in the scatter plot: if the variation in p_i results in a flat distribution of X_f, we can conclude that the given rate and

the given abundance are uncorrelated. This is the case depicted in the middle panel. On the other hand, if the variation in p_i results in a systematic change of X_f, the given rate and the given abundance are correlated. This is the situation shown in the right panel.

The ^{3}H(α,γ)^{7}Li and ^{3}He(α,γ)^{7}Be reaction rates have currently uncertainty factors of *f.u.* = 1.07 (i.e., 7%) and *f.u.* = 1.05 (i.e., 5%), respectively, at Big Bang nucleosynthesis temperatures. The strong impact of the latter reaction is easily explained because it directly produces ^{7}Be. The former reaction bypasses the synthesis of ^{7}Be and, furthermore, does not contribute to the direct synthesis of ^{7}Li because the produced ^{7}Li nuclei are quickly destroyed by the strong subsequent ^{7}Li(p,α)α reaction.

The identification of ^{3}He(α,γ)^{7}Be as the most important reaction impacting the nucleosynthesis of ^{7}Li is not surprising and could have been guessed without Monte Carlo procedures because the standard Big Bang nucleosynthesis network includes nuclides up to ^{7}Be and hence contains few reactions only. However, reaction networks for other astrophysical scenarios, for example, advanced and explosive burning stages in massive stars, binary star explosions (type Ia supernovae, classical novae, type I x-ray bursts), s-process, r-process, p-process, etc., contain several thousand nuclear interactions. Therefore, the identification of the most important reactions that impact a given isotopic abundance is not as obvious at first sight.

We have found the following procedure useful in several applications. Recall that the Monte Carlo study outputs the final abundances and rate variation factors for each sample network run. For each combination of nuclide and reaction a correlation factor is computed based on the scatter plot of final abundance versus rate variation factor. For a given nuclide, all reactions are then sorted in descending order according to the magnitude of the correlation factor. The reactions at the top of the list are the ones whose current rate uncertainties have the strongest impact on the nuclidic abundance.

When a linear correlation is known to be significant, the most commonly used correlation factor is Pearson's r [46], with values ranging from +1 to −1. It is defined for two variables, x_k and y_k, by the expression

$$r = \frac{\sum_k \left(x_k - \bar{x}\right)\left(y_k - \bar{y}\right)}{\sqrt{\sum_k (x_k - \bar{x})^2}\sqrt{\sum_k \left(y_k - \bar{y}\right)^2}}, \tag{5}$$

where $\bar{x}$ and $\bar{y}$ denote the mean values. If all the data lie on a perfect straight line, and the line has a positive slope, $r = +1$; for a negative slope, $r = -1$. These values hold independently of the magnitude of the slope. A value of r near zero indicates that no correlation exists. There are a number of disadvantages when using Pearson's r in connection with scatter plots of final abundance versus rate variation factor. First, it is well known that r is a poor statistic for deciding *whether* an observed correlation is statistically significant. Second, Pearson's r is a measure for a *linear* correlation between two variables. However, actual scatter plots frequently reveal non-linear correlations. This is demonstrated in figure 6, displaying a number of examples we have obtained for various scenarios: mass fraction ratio Si/H versus rate variation factor for ^{30}P(p,γ)^{31}S at the end of a classical nova simulation involving a 1.35 $M_\odot$ white dwarf [47] (left panel); final ^{15}N mass fraction versus rate variation factor for ^{18}O (α,n)^{21}Ne from supernova shock-induced nucleosynthesis. This occurs in the innermost region of the helium shell in a 15 $M_\odot$ massive star explosion model [48] (middle panel); and number abundance ratio CNO/H versus rate variation factor for ^{10}Be(p,α)^{6}Li in the context of an extended Big Bang nucleosynthesis network (right panel). None of these examples exhibit a linear correlation.

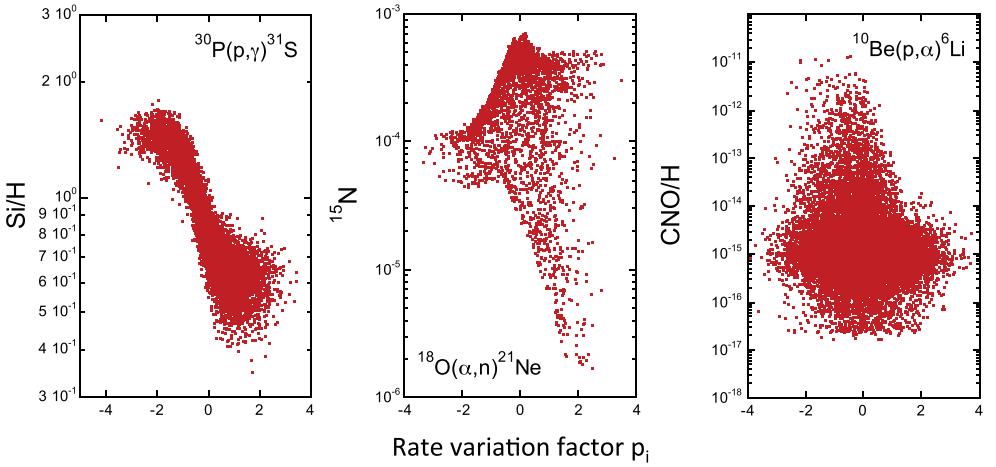

Figure 6. Results of Monte Carlo nucleosynthesis studies. (Left) Final mass fraction ratio of Si/H versus rate variation factor for ^{30}P(p,γ)^{31}S at the end of a classical nova simulation involving a 1.35 $M_\odot$ white dwarf. (Middle) Final mass fraction of ^{15}N versus rate variation factor for ^{18}O(α,n)^{21}Ne from from supernova shock-induced nucleosynthesis. (Right) Final number abundance ratio CNO/H versus rate variation factor for ^{10}Be(p,α)^{6}Li in the context of an extended Big Bang network (391 reactions).

A better choice is the Spearman rank-order correlation coefficient (r_s), which quantifies how well the relationship between two variables is described by a monotonic function. It is obtained from equation 5 when the actual values of x_i and y_i are replaced by their ranks. Values of $r_s = +1$ or $r_s = -1$ are obtained if the relationship between the two variables is given by a perfectly increasing or decreasing monotonic function, respectively. The Spearman coefficient is also more robust compared to Pearson's r in connection with outliers, in a similar sense that the median value of a distribution is more robust to outliers than the mean value.

For the scatter plots shown in figure 5, the Spearman coefficients amount to $r_s = 0.012$ (middle panel) and +0.69 (right panel), verifying that no correlation exists between the ^{7}Li/H ratio and the ^{3}H(α,γ)^{7}Li rate, and that the ^{7}Li/H ratio is correlated with the ^{3}He(α,γ)^{7}Be rate. For the scatter plot shown in the left panel of figure 6, we obtain $r_s = -0.86$. The Spearman coefficient correctly predicts a strong correlation because the relationship between the displayed variables is monotonic. For the middle panel, we obtain a small value of $r_s = 0.05$ and hence this case could be easily overlooked if the impact of reaction rates is quantified and ranked according to the magnitude of the correlation coefficient. Clearly, one has to be careful because the Spearman coefficient is not designed to quantify such a non-uniform, two-dimensional pattern.

Finally, for the right panel in figure 6 we obtain a value of $r_s = -0.213$, indicating a significant negative correlation between the number abundance ratio CNO/H and the ^{10}Be(p,α)^6 Li reaction rate for an extended Big Bang nucleosynthesis network. The Monte Carlo method results in a primordial range of CNO/H = $(4.94 - 28.5) \times 10^{-16}$ (68% coverage probability). It confirms earlier results [49], but provides in addition a meaningful uncertainty. Notice the tail towards higher values, CNO/H $>10^{-13}$, for which a small, but finite, probability is obtained (2%). This result could imply that some of the first-generation massive stars [50] do not need to self-produce as much CNO nuclei to meet their nuclear energy generation requirements. This region of the scatter plot is caused by the combination of higher sampled

rates for reactions that connect to the CNO region, chiefly ^{8}Li(t,n)^{10}Be and ^{10}Be(α,n)^{13}C, and lower sampled rates for reactions that return matter to the lightest nuclides, mainly ^{10}Be(p, α)^{7}Li and ^{10}Be(p,t)2α. Since these four reactions involving radioactive ^{10}Be have not been measured in the laboratory yet, the rates were estimated from theory (using TALYS). Thus we assign a factor uncertainty of *f.u.* = 100 to these reaction rates, which is a reasonable estimate for reactions among light nuclei at low energies. The identification of this potentially new path from Li towards the CNO region via ^{10}Be could not have been made if the rates were varied individually one-by-one in sequential network runs (i.e., without using the Monte Carlo method): individual variations of these rates by a factor of 1000 yield at most a 30% increase in CNO production!

4. Summary and conclusions

Statistical methods are necessary to improve estimates of both thermonuclear reaction rates and nucleosynthesis predicted by nuclear reaction networks. Experimental reaction rates can be estimated by using a Monte Carlo method once appropriate probability density functions are adopted for each nuclear physics input quantity. For example, resonance energies are best described by a Gaussian probability density, while for resonance strengths a lognormal probability density is more appropriate. Unobserved resonances of unknown strength can be easily incorporated into this framework by assuming a Porter–Thomas probability density. The random sampling over all nuclear input parameters produces in most cases a lognormal (output) reaction rate probability density. This function provides statistically rigorous recommended (median) reaction rates and factor uncertainties. We also discussed the usefulness of the Monte Carlo method for estimating the fractional contributions to the total reaction rate. Such calculations are important for the design of experiments at stable beam and radioactive ion beam facilities.

These results led directly to the construction of a next-generation nuclear reaction library, STARLIB, containing reaction rates, uncertainties, and rate probability densities for easy implementation into reaction networks for stellar models. STARLIB contains the necessary nuclear physics information to perform Monte Carlo nucleosynthesis simulations. All reaction rates can be sampled simultaneously, except for reverse reactions since these are related to the corresponding forward reaction rates via the reciprocity theorem. For the sampling of reaction rates, which are described by lognormal probability densities, we introduce a Gaussian random variable, p_i, for each each reaction, i. In the simplest case, it can be assumed that this *rate variation factor* is independent of temperature. The random factor by which a given sampled rate is modified from its median value is given by $(f.u.)^{p_i}$, which is temperature-dependent in any case through the factor uncertainty, *f.u.*

Finally, we discussed how to assess the impact of reaction rate uncertainties on the abundance of a given nuclide. Scatter plots displaying the final abundance, X_f, versus the rate variation factor, p_i, of reaction i are useful for quantifying correlations. We provide several examples that impact s-process neutron sources, core-collapse supernovae, classical novae, and Big Bang nucleosynthesis. The challenge is to identify which reactions, among typically several thousand in an extended network, have the largest impact on a given abundance. Useful results are obtained with the Spearman rank-order correlation coefficient, which is designed to quantify correlations for a monotonic relationship between two variables. We also gave examples for more complicated correlations that are not easily identified on the basis of the Spearman coefficient alone.

Acknowledgments

This work was supported in part by the National Science Foundation under award number AST-1008355 and by the US Department of Energy under Contracts No. DE-FG02-97ER41041 and DE-FG02-97ER41042.

References

[1] Abazajian K N *et al* 2009 The seventh data release of the Sloan digital sky survey *Astrophys. J. Suppl. Ser.* **182** 543–58
[2] Rau A *et al* 2009 Exploring the optical transient sky with the Palomar transient factory *Publ. Astron. Soc. Pac.* **121** 1334–51
[3] Law N M *et al* 2009 The Palomar transient factory: system overview, performance, and first results *Publ. Astron. Soc. Pac.* **121** 1395–408
[4] Koch D G *et al* 2010 Kepler mission design realized photometric performance, and early science *Astrophys. J.* **713** 79–86
[5] Batalha N M *et al* 2010 Selection prioritization, and characteristics of Kepler target stars *Astrophys. J.* **713** 109–14
[6] Paxton B, Bildsten L, Dotter A, Herwig F, Lesaffre P and Timmes F 2011 Modules for experiments in stellar astrophysics (MESA) *Astrophys. J. Suppl. Ser.* **192** 3
[7] Paxton B *et al* 2013 Modules for experiments in stellar astrophysics (MESA): planets, oscillations, rotation, and massive stars *Astrophys. J. Suppl. Ser.* **208** 4
[8] Balantekin A B *et al* 2014 Nuclear theory and science of the facility for rare isotope beams *Mod. Phys. Lett.* A **29** 30010
[9] Cesaratto J M, Champagne A E, Clegg T B, Buckner M Q, Runkle R C and Stefan A 2010 Nuclear astrophysics studies at LENA: the accelerators *Nucl. Instrum. Methods Phys. Res.* A **623** 888–94
[10] Longland R, Iliadis C, Champagne A E, Fox C and Newton J R 2006 Nuclear astrophysics studies at the LENA facility: the γ-ray detection system *Nucl. Instrum. Methods Phys. Res.* A **566** 452–64
[11] Caughlan G R and Fowler W A 1988 Thermonuclear reaction rates V *At. Data Nucl. Data Tables* **40** 283
[12] Angulo C *et al* 1999 A compilation of charged-particle induced thermonuclear reaction rates *Nucl. Phys.* A **656** 3–183
[13] Iliadis C, D'Auria J M, Starrfield S, Thompson W J and Wiescher M 2001 Proton-induced thermonuclear reaction rates for A = 20–40 nuclei *Astrophys. J. Suppl. Ser.* **134** 151–71
[14] Smith D L, Naberejnev D G and van Wormer L A 2002 Large errors and severe conditions *Nucl. Instrum. Methods* A **488** 342–61
[15] Longland R, Iliadis C, Champagne A E, Newton J R, Ugalde C, Coc A and Fitzgerald R 2010 Charged-particle thermonuclear reaction rates: I. Monte Carlo method and statistical distributions *Nucl. Phys.* A **841** 1–30
[16] Iliadis C, Longland R, Champagne A E, Coc A and Fitzgerald R 2010 Charged-particle thermonuclear reaction rates: II. Tables and graphs of reaction rates and probability density functions *Nucl. Phys.* A **841** 31–250
[17] Iliadis C, Longland R, Champagne A E and Coc A 2010 Charged-particle thermonuclear reaction rates: III. Nuclear physics input *Nucl. Phys.* A **841** 251–322
[18] Iliadis C, Longland R, Champagne A E and Coc A 2010 Charged-particle thermonuclear reaction rates: IV. Comparison to previous work *Nucl. Phys.* A **841** 323–88
[19] Longland R, Iliadis C and Karakas A 2012 Reaction rates for the s-process neutron source ^{22}Ne + α *Phys. Rev.* C **85** 065809
[20] Iliadis C 1997 Proton single-particle reduced widths for unbound states *Nucl. Phys.* A **618** 166–75
[21] Porter C E and Thomas R G 1956 Fluctiations of nuclear reaction widths *Phys. Rev.* **104** 483
[22] Pogrebnyak I, Howard C, Iliadis C, Longland R and Mitchell G E 2013 Mean proton and α-particle reduced widths of the Porter–Thomas distribution and astrophysical applications *Phys. Rev.* C **88** 015808

[23] Woosley S E, Arnett W D and Clayton D D 1973 The explosive burning of oxygen and silicon *Astrophys. J. Suppl.* **26** 231
[24] Woosley S E and Hoffman R D 1992 The alpha-process and the r-process *Astrophys. J.* **395** 202–39
[25] Timmes F X, Woosley S E, Hartmann D H and Hoffman R D 1996 The production of ^{44}Ti and ^{60}Co in supernovae *Astrophys. J.* **464** 332
[26] The L-S, Clayton D D, Jin L and Meyer B S 1998 Nuclear reactions governing the nucleosynthesis of 44Ti *Astrophys. J.* **504** 500
[27] Hoffman R D *et al* 2010 Reaction rate sensitivity of ^{44}Ti production in massive stars and implications of a thick target yield measurement of ^{40}Ca(α, γ)^{44}Ti *Astrophys. J.* **715** 1383–99
[28] Magkotsios G, Timmes F X, Hungerford A L, Fryer C L, Young P A and Wiescher M 2010 Trends in ^{44}Ti and ^{56}Ni from core-collapse supernovae *Astrophys. J. Suppl. Ser.* **191** 66–95
[29] Larsson J *et al* 2011 X-ray illumination of the ejecta of supernova 1987 A *Nature* **474** 484–6
[30] Grebenev S A, Lutovinov A A, Tsygankov S S and Winkler C 2012 Hard-x-ray emission lines from the decay of ^{44}Ti in the remnant of supernova 1987 A *Nature* **490** 373–5
[31] Robertson D, Görres J, Collon P, Wiescher M and Becker H-W 2012 New measurement of the astrophysically important ^{40}Ca(α,γ)^{44}Ti reaction *Phys. Rev.* C **85** 045810
[32] Iliadis C 2007 *Nuclear Physics of Stars* (New York: Wiley)
[33] Newton J, Iliadis C, Champagne A, Coc A, Parpottas Y and Ugalde C 2007 Gamow peak in thermonuclear reactions at high temperatures *Phys. Rev.* C **75** 045801
[34] Rauscher T 2010 Relevant energy ranges for astrophysical reaction rates *Phys. Rev.* C **81** 045807
[35] Jose J and Hernanz M 2007 The origin of presolar nova grains *Meteorit. Planet. Sci.* **42** 1135–43
[36] Sallaska A L, Iliadis C, Champange A E, Goriely S, Starrfield S and Timmes F X 2013 STARLIB: a Next-generation reaction-rate library for nuclear astrophysics *Astrophys. J. Suppl. Ser.* **207** 18
[37] Cyburt R H *et al* 2010 The JINA REACLIB database: its recent updates and impact on type-I x-ray bursts *Astrophys. J. Suppl. Ser.* **189** 240–52
[38] Aikawa M, Arnould M, Goriely S, Jorissen A and Takahashi K 2005 BRUSLIB and NETGEN: the Brussels nuclear reaction rate library and nuclear network generator for astrophysics *Astron. Astrophys.* **441** 1195–203
[39] Stoesz J A and Herwig F 2003 Oxygen isotopic ratios in first dredge-up red giant stars and nuclear reaction rate uncertainties revisited *Mon. Not. R. Astron. Soc.* **340** 763
[40] Parikh A *et al* 2008 The effects of variations in nuclear processes on type I x-ray burst nucleosynthesis *Astrophys. J. Suppl. Ser.* **178** 110
[41] Roberts L F, Hix R W, Smith M M and Fisker J L L Monte Carlo simulations of type I x-ray burst nucleosynthesis *Proc. Science (CERN, February 2006)* pp 1–6
[42] Longland R 2012 Recommendations for Monte Carlo nucleosynthesis sampling *Astron. Astrophys.* **548** A30
[43] Cyburt R H, Fields B D and Olive K A 2008 An update on the Big Bang nucleosynthesis prediction for ^{7}Li:the problem worsens *J. Cosmol. Astropart. Phys.* JCAP11(2008)012
[44] Fields B D 2011 The Primordial lithium problem *Annu. Rev. Nucl. Part. Sci.* **61** 47–68
[45] Coc A, Goriely S, Xu Yi, Saimpert M and Vangioni E 2011 Standard Big Bang nucleosynthesis up to CNO with an improved extended nuclear network *Astrophys. J* **744** 158
[46] Press W H, Teukolsky S A, Vetterling W T and Flannery B P 1992 *Numerical Recipes in FORTRAN. The Art of Scientific Computing* 2nd edn (Cambridge: Cambridge University Press)
[47] Kelly K J, Iliadis C, Downen L, Jose J and Champagne A 2013 Nuclear mixing meters for classical novae *Astrophys. J.* **777** 130
[48] Meyer B S and Bojazi M J 2013 Sensitivity of nitrogen-15 production in explosive helium burning to supernova energies and reaction rates and importance for low-density supernova graphite grains *Lunar and Planetary Science Conf.* vol 44 p 3006 Lunar and Planetary Inst. Technical Report
[49] Iocco F, Mangano G, Miele G, Pisanti O and Serpico P 2007 Path to metallicity: synthesis of CNO elements in standard BBN *Phys. Rev.* D **75** 087304
[50] Ekström S, Meynet G, Chiappini C, Hirschi R and Maeder A 2008 Effects of rotation on the evolution of primordial stars *Astron. Astrophys.* **489** 685–98
[51] Champagne A E, Iliadis C and Longland R 2014 *AIP Adv.* **4** 041006